Zeitschrift: Helvetica Physica Acta
Band: 46 (1973)
Heft: 6

Artikel: An analysis of the neutrino elastic (+np+^-) events
Autor: Yoshiki, H.
DOI: https://doi.org/10.5169/seals-114511

Helvetica Physica Acta
Vol. 46, 1974. Birkhäuser Verlag Basel

An Analysis of the Neutrino Elastic ($\nu+n\to p+\mu^-$) Events[1]

by **H. Yoshiki**

National Laboratory for High Energy Physics, Oho-machi, Tsukuba-gun, Ibaraki-ken, 300-32, Japan

(22. VIII. 73)

Abstract. An enhancement in μp mass-spectrum at 1.8–2.0 Gev/c^2 mass region from the elastic neutrino reaction, $\nu + n \to p + \mu^-$, is discussed. The observation is based on the CERN neutrino experiments from 1963 to 1967 using the CERN Heavy Liquid Bubble Chamber.

1. Introduction

The effect of μp mass enhancement has been published in 1969 [10] on the basis of 1967 propane runs. The present paper is to give minute accounts of the analysis in Ref. [10]. It contains also the results of the 1963 (freon) run. The details of the experimental procedures can be found in previously published papers [4, 5, 10, 11] and the related articles thereof. The data collected have been summarized in Data Summary Tapes (DST) by the neutrino experimental group and the events used for the present analysis (as well as for Ref. [10]) are extracted from those DSTs. The selection was made according to the rules described in Section 3.

In events containing a μ^- and a single proton of any momentum, an enhancement of approximately three standard deviations is observed in the μ^-p invariant mass distribution in the 1.8 to 2.0 GeV/c^2 mass region. The mass error in this region is typically about $\pm$50 MeV/c^2. In order to increase the statistics, no fiducial volume cut is applied. If this effect is not a statistical fluctuation, but is due to a μp resonant state, then the experimentally observed cross-section and width imply that the life-time is $\sim 10^{-12}$ sec. The cross-section observed is $\sim 10^{-6}$ of that predicted for the production of a scalar boson of the same mass mediating the weak interaction. The best estimate of the mass, based on the propane data, is 1.94 $\pm$ 0.06 GeV/c^2, and 1.85 $\pm$ 0.08 for freon, where the quoted errors include estimates of possible systematic errors. The average of the two gives 1.91 $\pm$ 0.05 GeV/c^2. The forward-peaked muon distribution in the centre-of-mass system excludes a spin-zero assignment.

2. Theoretical Background

The weak interaction can be described by an interaction Lagrangian

$$\mathscr{L} = (G/\sqrt{2})\,(J^h_\mu + J^l_\mu)^\dagger\,(J^h_\mu + J^l_\mu), \tag{2.1}$$

[1]) The original version of this article is TC-L/Int. 69-21, CERN (1969).

where

$$G = 10^{-5}/m^2, \tag{2.2}$$

m is the nucleon mass. J^l_μ is the leptonic current,

$$J^l_\mu = \bar{e}\gamma_\mu(1+\gamma_5)\,\nu_e + \bar{\mu}\gamma_\mu(1+\gamma_5)\,\nu_\mu \tag{2.3}$$

where e, ν_e, μ and ν_μ stand for the fields associated with the electron, electron–neutrino, muon and muon–neutrino respectively and the γ's are the usual Dirac matrices [1]. J^h_μ is the hadronic current operator. Although the knowledge of its structure increased greatly during the past decade, in the absence of the strong interactions, it may be written like (2.3) [2]. For nuclear β-decay for instance,

$$J^h_\mu = \bar{p}\gamma_\mu(1+\gamma_5)\,n \tag{2.4}$$

will couple to the first term of (2.3).

From the phenomenological analysis of the weak interaction in leptonic, semi-leptonic and non-leptonic decays, the existence of an intermediate charged vector boson exchanged in the t-channel has long been predicted [3]. High energy experiments have not detected this particle, the present measured lower limit for its mass being 1.8 GeV with 99% confidence level [4, 5]. Current theoretical estimates of its mass range from 3 to 8 GeV [6].

Several authors [7, 8] have attempted to ensure the renormalizability of the theory by introducing a scalar intermediate boson instead. By a Fierz transformation, one can show that

$$\begin{aligned}\mathscr{L} &= (G/\sqrt{2})\,\bar{p}\gamma_\mu(1+\gamma_5)\,n\bar{\mu}\gamma_\mu(1+\gamma_5)\,n,\\ &= (2G/\sqrt{2})\,\bar{p}(1-\gamma_5)\mu^c\,\bar{\nu}^c_\mu(1-\gamma_5)\,n,\end{aligned} \tag{2.5}$$

which indicates the possibility of exchanging a scalar particle in the s-channel. These authors claimed that such a boson should be observable in neutrino reactions as a resonance between the muon–neutrino and the neutron. In that case the calculation shows that we should observe it about 10^6 times stronger (taking into account all smearing effects) than the ordinary non-resonant process. No such phenomenon has been observed for boson masses below 6 GeV [4, 9, 10]. A possible remedy for this is to assume two coupling constants, g for the neutron–neutrino vertex and g' for the muon–proton vertex [8]. However, as will be discussed below, the experimental facts do not favour this idea either. 'Deception' is the terminology of Gell-Mann et al. for schemes of this kind [6].

3. Selection of Events

We have selected events containing only a μ^- candidate and just one possible secondary proton of any length. A blob was counted as a proton. Events with associated visible neutrals (neutron or gamma-rays) were rejected. The events retained were classed as either 'μp' or 'μC' events according to whether or not the proton could be positively identified as such, by range, curvature and ionization. The 'μC' events, typically consisting of a non-interacting negative track (μ^-) and a fast positive track that leaves the chamber, thus contain some events in which the 'proton' is really a π^+.

The total numbers of such events, in the full volume of the chamber, were 181 in propane (of which 34% are μC) and 165 in freon (16% μC). These 346 events were subjected to the following tests:

1) The resultant secondary momentum observed along the neutrino direction, $\sum p_x$, must exceed 0.3 GeV/c.[2])
2) $Q^2 < Q^2_{\max}$; the observed 4-momentum transfer squared,

$$Q^2 = 2E_{\text{vis}}(E_\mu - p_{\mu x}) - m_\mu^2, \tag{3.1}$$

where E_{vis} is the visible energy released in the chamber, E_μ the total energy of the muon, $p_{\mu x}$ the muon momentum in the direction of the neutrino and m_μ the muon rest mass, must be smaller than the *maximum* value $Q^2_{\max}$ kinematically possible for the elastic process. $Q^2_{\max}$ is well defined if the target is at rest. But under the influence of the Fermi motion we can only predict it to lie in a certain band. We have chosen the minimum value in the band

$$Q^2_{\max} = \frac{4(\sqrt{m_n^2 + p_f^2} - p_f)^2 E^2_{\text{vis}}}{m_n^2 + 2(\sqrt{m_n^2 + p_f^2} - p_f)\, E_{\text{vis}}} \tag{3.2}$$

in order to be conservative. Here p_f is the Fermi momentum and was taken as 250 MeV/c.

3) $0.48 < M^{*2} < 1.28$ GeV^2; the square of the missing mass,

$$M^{*2} = m_n^2 + 2m_n(E_{\text{vis}} - E_\mu) - Q^2, \tag{3.3}$$

where m_n is the neutron mass, must lie within $\pm$ 0.40 GeV^2 of the square of the proton mass (0.88 GeV^2).[3])

The first test, supplemented by the second, removes most of the background events due to interactions of incoming neutrons and pions [11]. The third test, the effect of which is illustrated in Figure 1, tests the elasticity of the event and rejects in particular most of the inelastic events in which the pion produced is reabsorbed in the same nucleus. Other variations on these tests have also been employed.[2,3]

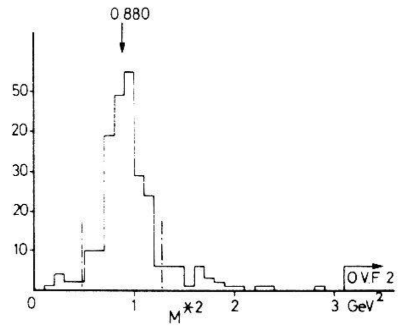

Figure 1
Distribution of M^{*2}, square of missing mass, after tests (1) and (2). Broken lines are the limits given by test (3).

---

[2]) In Ref. [23d], events with either $\sum p_x > 0.2$ GeV/c or $E_{\text{vis}} < 0.5$ GeV were accepted.

[3]) Due to the Fermi motion of the target, the elastic events are distributed in an allowed area in $M^{*2} - Q^2$ plane. By a Monte Carlo method the following expression was obtained for an estimate of the allowed region of M^{*2}, $M^{*2} \lesssim 0.88 \pm (0.23Q^2 + 0.15)$. This is a more severe test than (3) if Q^2 is below 1.1 GeV/c^2. In Ref. [10] (3) was replaced by this test.

These tests reduce the 346 original events to 221 events, of which 130 are in propane, and 91 in freon, and the fractions of C events reduce to 20% and 8% respectively.

4. The Monte Carlo Calculation

Since the elastic neutrino events occur only in complex nuclei, it is necessary to study the nuclear effect on the produced protons, since their final kinematics are related to various quantities of interest. To this end, we performed a Monte Carlo calculation with a very simple nuclear model, which is justified because we are dealing with protons of large energies compared to the binding energy of nucleons inside the nucleus.

The Monte Carlo program consisted of the following four parts: (a) generation of elastic events, (b) tracing the proton produced inside the nucleus, (c) classification of the events and (d) introduction of the tests and production of histograms. The following procedure was employed:

a) The cross-sections calculated by several authors [13] are used to generate neutrino 'events' by the Monte Carlo program. The neutrino spectrum based on yield data [14] of pions and kaons from the target material of the neutrino horn [15] was used as the input for the freon data. The shape of the spectrum is considered to be much more accurate than the absolute uncertainty of $\pm$ 30%. For the propane data, the flux was also computed [16] from measurements of the muon range distribution in the neutrino shield, which was continuously monitored during the runs. Above 1 GeV, the absolute flux estimate is considered accurate to $\pm$ 15%. However, this method fails to give the spectrum accurately below 1 GeV, where the result of the previous method was continued. We have used only the relative shape of the spectra throughout the calculation. The axial form factor F_A is assumed to be of the double-pole form. The induced pseudo-scalar term, F_p, is ignored. $M_V = 0.84$ GeV/c^2, $\lambda = 1.23$ and $\mu = 3.71$ are used respectively. A number of runs were repeated with various values of M_A and in this paper we present the results for $M_A = 0.8$ GeV/c^2. The upper limit to the Fermi momentum is taken as 250 MeV/c.

b) Treating the nucleus as a degenerate Fermi gas, the fate of the produced protons is traced in a cascade program, similar to that used by Myatt and by Franzinetti and Manfredotti [17]. Improvements were made in the nucleon–nucleon collision cross-section by using more recent data compiled by, e.g., Kazarinov, Wilson, Cheng, Lomon and Feschbach [18]. The cross-sections and angular distributions were not parameterized but the measured values were directly folded into the program as data. Data on single pion production in nucleon–nucleon collisions were compiled and these were used as input data. The production mechanism in complex nuclei is assumed to be similar to that suggested by Chew and Steinberger [19]. The result reproduces the π^+/π^- ratio for different proton energies surprisingly well. It is also consistent with Sidorov's pion spectra [20] measured at 660 MeV protons energy. With this, and one variable parameter matched to the measured cross-sections at lower energies [21], it was considered that pion production in nucleon–nucleon collisions inside a complex nucleus could be very well represented. A square well potential of depth 40 MeV and a nuclear radius of 1.3 $A^{1/3}$ Fermi were assumed. The results were found to be not strongly dependent on the values used.

c) The events are classified into (1) cases prohibited by the Pauli principle, (2) cases of pion production and (3) other cases, further classified, according to the number of protons and neutrons actually emerging from the nuclear surface.

d) The tests described in the previous section were imposed on the one proton prong events thus generated. Those which passed the tests are stored in a histogram plotting routine, then sorted and printed as required.

We omit detailed discussions of the results of this calculation here. Instead, we compare the results with observed distributions to check the general correctness of the calculation. We take a weighted average of the results for propane and freon according to the relative total numbers of events observed. Figure 2 shows the observed distributions of E_{vis}, p_p, p_μ and Q^2. The Monte-Carlo predictions, normalized to the total number of events, are indicated by dots. Curves are drawn smoothly connecting these dots. The forms of the curves satisfactorily follow the observations, thus verifying the reliability of the Monte Carlo calculation.

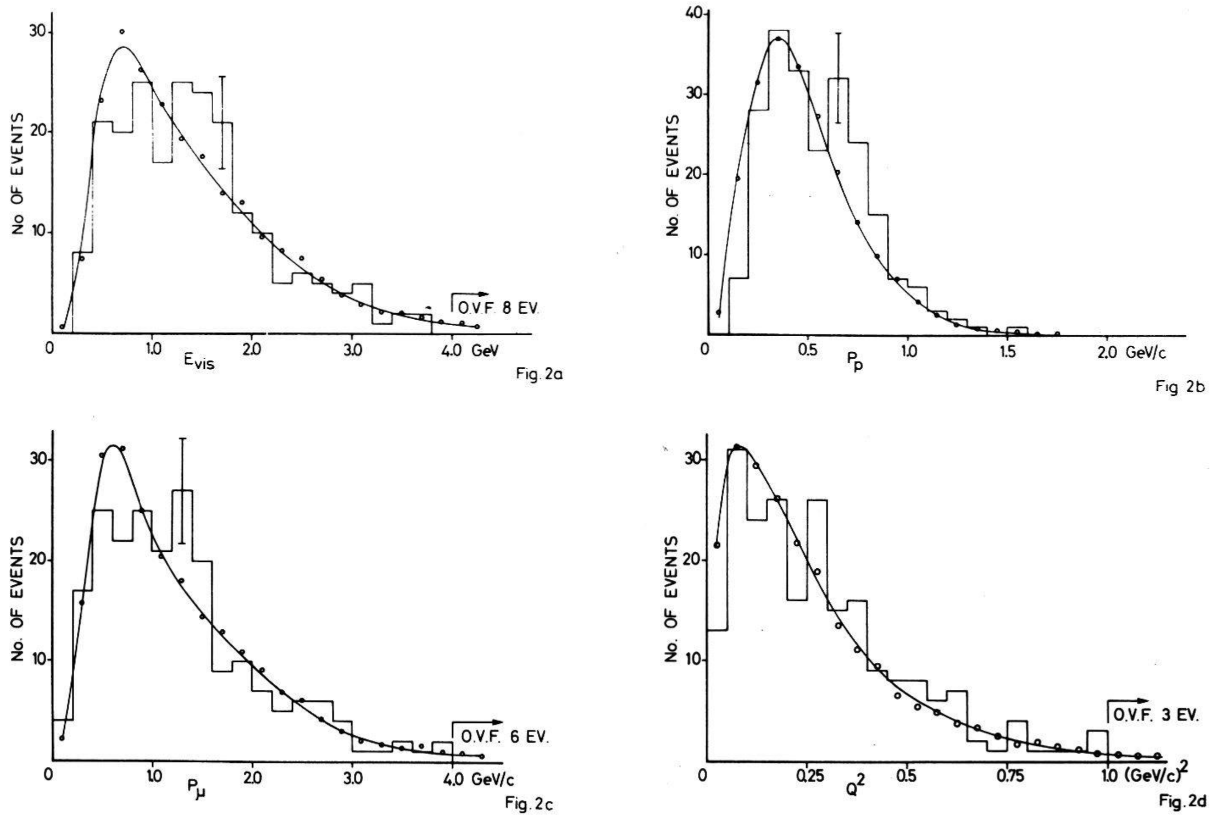

Figure 2
Observed distributions of (a) E_{vis}, (b) p_p, (c) p_μ and (d) Q^2 with the results of the Monte Carlo calculation.

In the following, the percentages quoted are arithmetic averages of the predictions for freon and propane. Among the elastic reactions taking place inside the nucleus, 6% give pions in subsequent interactions. The remaining 94% are non-mesonic with various numbers of protons and neutrons emitted. In the non-mesonic category, 70% are one-proton events with an arbitrary number of neutrons. Our sample corresponds to this group. In this group, 39% are accompanied by secondary neutrons or by protons trapped in the nucleus. The remaining 61% are the so-called 'genuine' events, where a proton emerges from the nucleus without any collision, although the potential may refract it at the nuclear surface. This refraction was disregarded in our calculation. The tests in fact increase the fraction of genuine events among the one-proton prong events by only a few per cent. Some of the events with associated neutrons were eliminated from our sample because the neutrons were detected. If one takes this into account, 89% of the selected μp events in freon would be genuine, and 73% of those in propane.

5. Backgrounds

a) μC events containing a π^+

Some $n\pi^+\mu$ events which, according to Adler [22], occur one-quarter as often as $p\pi^+\mu$, are accepted as μC events if the neutron is undetected and the π^+ unidentified. Monte Carlo $n\pi^+\mu$ events were generated with a target in Fermi motion, via the N^* (1236) state ($\Gamma = 0.11$). Then Monte Carlo elastic $p\mu$ events were generated and the proton then interpreted as a π^+. Errors assigned to the generated tracks were determined from the actual μC events. The kinematics of the unseen neutron were then recalculated assuming the target to have been at rest in the same way as for real events.

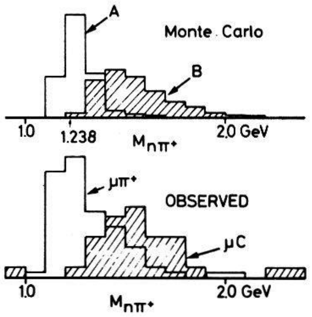

Figure 3
Comparison between the Monte Carlo calculation and the $\mu\pi^+$ and μC events.

The resultant $n - \pi^+$ invariant mass distributions from these two Monte Carlo calculations are shown as A and B in Figure 3. These distributions may be compared with the corresponding distributions obtained from a sample of observed $\mu\pi^+$ events, where the π^+ was identified and all momenta well measured, and the actual μC samples in our data shown in the lower part of Figure 3.

The comparison indicates that the majority of μC events are in fact μp, since the distribution of real μC events resembles histogram B rather than A. This conclusion is also supported (1) by the fact that the high momentum tail of the p_p spectrum (Fig. 2) consists mainly of μC events and is in good agreement with and not *in excess* of the cascade Monte Carlo calculation (the dots) and (2) the results of δ-ray analysis indication that $\sim 90\%$ of all ambiguous tracks are protons [10].

b) Background from $p\pi^+\mu$ events where the π^+ is reabsorbed in the nucleus

This has a negligible effect for the one-proton events since the π^+ reabsorption without any visible proton takes place less than 2% of the time of the total π^+ production [17c].

c) $\mu^- p\pi^0$ events with undetected π^0

If the neutral pion is undetected, kinematical separation between $p\mu$ and $p\pi^0\mu$ events is very difficult because the maximum transverse momentum of the $p\pi^0$ system of N^* is of the same order of magnitude as the Fermi momentum unbalance. Various Monte Carlo calculations demonstrate this fact. The M^{*2} test, for instance, hardly distinguishes $p\pi^0\mu$ from $p\mu$ even at $Q^2 \sim 0$, and the quantities derived from $p\pi^0\mu$

events assuming an unseen π^0 are distributed widely through the elastic region. We can therefore only estimate the $p\pi^0\mu$ background in our sample, not eliminate it.

In the propane data, from the 11 observed $p\mu$ events with one or two associated gamma rays which pass our tests if the gammas are ignored, we may calculate the expected number of $p\pi^0\mu$ events with no detected gamma present in our sample. After allowing for pion absorption charge exchange in the nucleus, and gamma escape probabilities, we thus estimate this background as 9 ± 4 events. Another way to estimate it is to convert the number of observed $p\pi^+\mu$ events on free protons [11] to the number of $p\pi^0\mu$ events, supposing that N^* production is the dominant mode [22]. Including all corrections, this estimate yields 10 ± 3 expected background events.

The $p\pi^0\mu$ background in the freon data is negligible compared to that in propane because the radiation length of the liquid is ten times shorter. Therefore we conclude that the total background of $p\pi^0\mu$ events is about $4 \pm 2\%$.

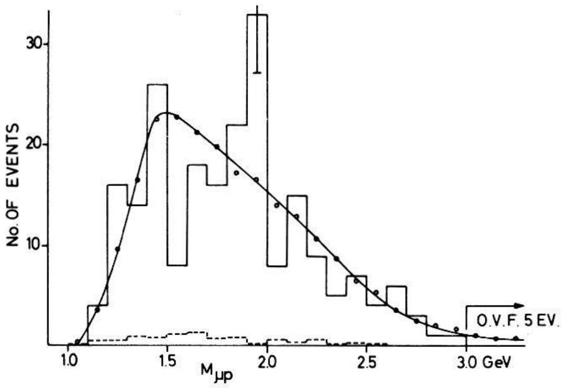

Figure 4
Muon–proton invariant mass distribution after the tests. The broken lines indicate expected background from $p\pi^0\mu$ events.

Expected μp invariant mass spectrum of the background is that of $p\pi^+\mu$ where the pions are assumed to be non-existent. After the tests, it has a single broad peak around 1.6 GeV, (broken lines in Fig. 4).

d) Summary

The background of events that are not due to the process $\nu + n \to p + \mu$ is small in our sample. Furthermore, the μp mass distribution of background events are broad and not greatly different from that expected from the ordinary elastic process. Thus, for the purpose of the present analysis, the background can safely be ignored.

6. The Mass Spectrum

Figure 4 shows a histogram of muon–proton invariant mass with tests and with 100 MeV bin size starting from 1.0 GeV. From 1.8–2.0 GeV one observed an enhancement of about three standard deviations above the Monte Carlo prediction. Or, more precisely, 55 events were observed against 33 expected between 1.8 and 2.0 GeV, namely the observed is 3.8 standard deviations in excess of the expected number. This effect has been reported already elsewhere but with different tests. Notwithstanding those changes the effect has always been observed [10–23].

However, we must also take into account the uncertainty in the prediction that 33 events are expected. Since this prediction is based on the shape of the neutrino flux, which was estimated differently for the freon and propane data, we are forced to consider the freon and propane data separately. Figure 7 illustrates the relationship between $\mu^- p$ invariant mass and neutrino energy. In the propane run, the muon flux was continuously monitored in order to determine the neutrino spectrum. The method permits more accurate spectrum determination in high energy part. This is because the high energy muons can only be detected deep in the shield, where the contamination

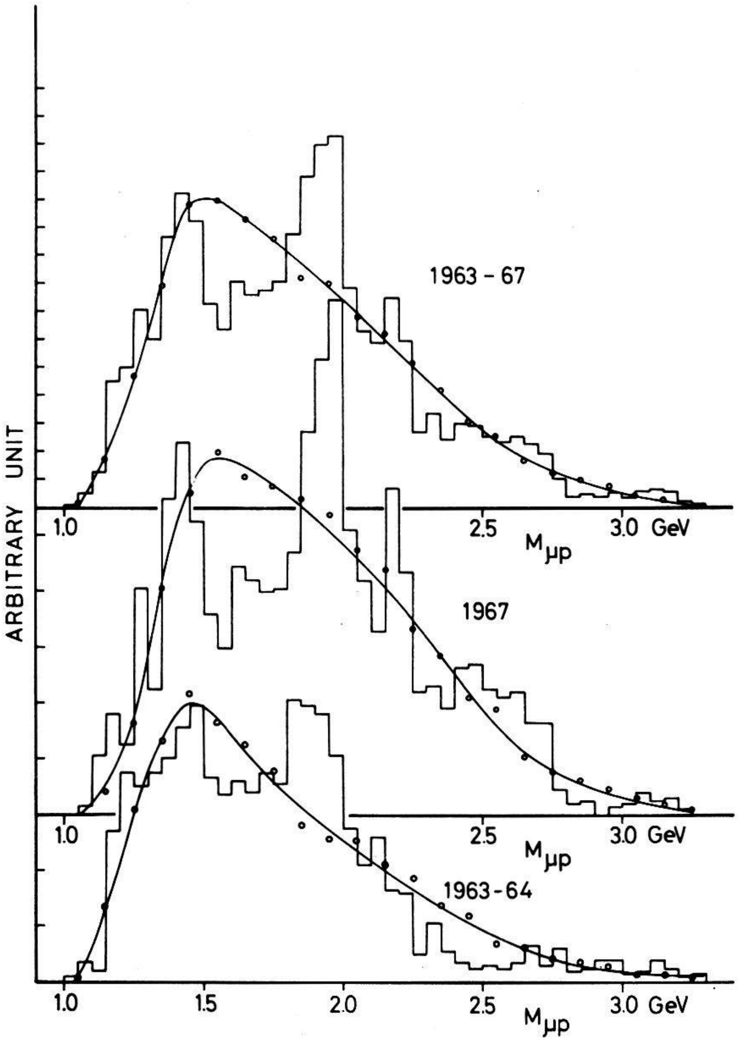

Figure 5
Muon–proton invariant mass distribution after the observed events are distorted. Note one unit of ordinate corresponds to an event per 50 MeV and the widths are wider by a factor of $\sqrt{2}$ than the undistorted histogram.

of hadrons is negligible, and high energy muons correspond to high energy neutrinos. Thus, while the shape of the neutrino spectrum above 2 GeV is determined directly and rather precisely ($\pm$ 3%) the continuation of this shape to lower energies is based on an extrapolation to lower pion momenta of the parent pion spectrum deduced from the muon measurements. Consequently, the ratio of the flux in the 1–2 GeV region to that above 2 GeV is known only within $\pm$ 10%. In the freon runs, the flux can only be estimated directly from the pion production spectrum and the corresponding uncertainty is rather higher (about $\pm$ 20%). The uncertainty in the expected number of events due to the uncertainty in the neutrino flux is therefore believed to be $\pm$ 4.5 events. Including the statistical error in the expected number, 55 events are observed where 33 $\pm$ 7.3 should be expected and the effect remains at the three standard deviation levels.

Figure 5 shows an 'ideogram' of the data prepared in the following way. For each of the 346 observed events containing a μ^- and single proton, including those rejected by the cuts, 20 distorted events were generated. The distortion is based on the quoted errors from GRIND in the dip, azimuthal angle and momentum of each track. Each such distorted event was then subjected to the tests employed for the real events and plotted if it passed the tests. This method has the advantage over the ordinary ideogramming procedure of automatically weighing appropriately any badly measured events or events close to the cuts, and of giving better estimates of the errors in quantities where the ordinary linear propagation of errors is inadequate because of the large errors in the measured quantities.

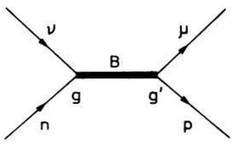

Figure 6
Production and decay of the B boson.

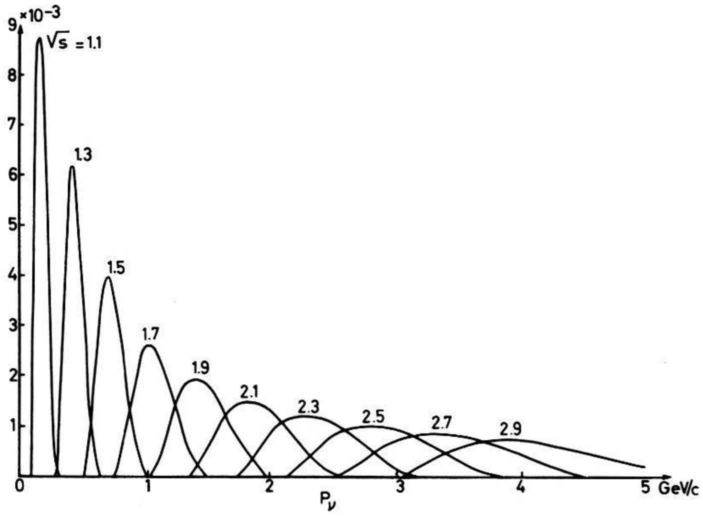

Figure 7
When a resonance is 1 MeV wide and a unit high, attenuation in height and increase in energy width of incoming neutrinos which associate to the resonance, due to the Fermi motion of the target, is shown. $\sqrt{s}$ is the resonance energy in GeV.

Using this procedure, the average error in the μp invariant mass in the 1.8 to 2.0 GeV/c^2 band is found to be $\pm$ 76 MeV in freon and $\pm$ 49 MeV in propane. This compares with 20 MeV for the N^* (1236) in propane, for which the Q-value is lower. If this effect is attributed to a new type of resonance B between the neutron and the muon–neutrino (Fig. 6) which decays into proton and muon, the estimate of the mass is 1.85 $\pm$ 0.08 GeV from the freon data and 1.94 $\pm$ 0.06 GeV from the propane data, the average of which gives 1.91 $\pm$ 0.05 GeV. In this case, as discussed in Section 9, the peak cross-section is given by $(J + \frac{1}{2})\pi\lambda\!\!\!^{-2}$ and is therefore of the order of 10^{-27} cm^2. The true width, Γ, must therefore be of the order $(\sigma_{\text{observed}}/10^{-27}\ \text{cm}^2) \times \Gamma_{\text{observed}} = 10^{-3}$ eV. This corresponds to a life-time of the order of 10^{-12} sec so that B decays freely outside the nucleus.

A corresponding effect can be also seen in the E_{vis} distribution in Figure 2(a) between 1 and 2 GeV although it is smeared out by the Fermi motion. For example, for a neutron of Fermi momentum 200 MeV/c parallel or antiparallel to the neutrino direction, centre of mass energy of 1.9 GeV corresponds to a neutrino energy of either 1.2 or 1.8 GeV. Conversely, because of the extremely narrow width of the resonance and the correspondingly small probability of encountering a neutron of the appropriate Fermi momentum, the average cross-section for production of such a resonance by a neutrino of about 1.5 ± 0.3 GeV, per nucleon in a complex nucleus, is only of the order of 10^{-39} cm^2. Thus the neutrinos can traverse the shield without being absorbed by the resonance production.

7. Angular Distribution

The angular distribution of the μ and p in the centre of mass system in the 1.8–2.0 GeV mass range is neither isotropic nor symmetric. It is very tempting to study it in more detail, although the number of events is limited, and this is the aim of the present section.

Table I

$m_{\mu p}$ (GeV)	$\lvert\vec{p}_t\rvert > 0.25$ GeV/c A†	$P(O)/P(A)$‡	α§	$\lvert\vec{p}_t\rvert < 0.25$ GeV/c A†	$P(O)/P(A)$‡	α§
1.0–1.4	0.158	0.81	0.24	−0.200	0.79	0.22
1.4–1.6	0.000	1.00	0.50	−0.111	0.94	0.36
1.6–1.8	−0.400	0.43	0.11	0.250	0.44	0.11
1.8–2.0	0.500	0.07	0.01	0.029	1.00	0.42
2.0–2.2	−0.111	0.96	0.38	−0.285	0.55	0.16
2.2–∞	0.000	1.00	0.50	0.200	0.62	0.17

†) Most likely value of $A = (N_+ - N_-)/(N_+ + N_-)$.
‡) Ratio of probability of A being zero to probability of A being most likely.
§) Probability of A being opposite in sign to the observation.

The Monte Carlo calculation described in Section 3 indicates that the distribution of the transverse momentum unbalance $|\vec{p}_t|$ in one-proton events drops sharply between 180 and 280 MeV/c, 80% of events having $|\vec{p}_t|$ below 250 MeV/c. Here $\vec{p}_t$ is the component of the total secondary momentum $\vec{p}_{tot}$ $(= \vec{p}_p + \vec{p}_\mu)$ perpendicular to the neutrino direction (which is defined within $\pm 0.5°$ by beam optics). There is also a tail up to 800 MeV/c due to secondary interactions of produced protons. In the real events, however, the fraction below 250 MeV/c is only 70% and the drop is less steep because of measurement errors, the diffused boundary of the Fermi momentum distribution and the optical properties of the nucleus, which we did not take into account.

These facts are related to the following observations. Consider the vector $\vec{\nu} \times \vec{p}_{tot}$, where $\vec{\nu}$ is the neutrino momentum. Generally $\vec{\nu}$ and $\vec{p}_{tot}$ are not parallel to each other because of the movement of the target neutron and of the secondary interaction of the produced proton in the nucleus. We count the numbers of events N_+ and N_- in which $\vec{p}_p \cdot (\vec{\nu} \times \vec{p}_{tot})$ is positive and negative respectively. The result, expressed in terms of the parameter $A = (N_+ - N_-)/(N_+ + N_-)$, is given in Table I. One immediately notices, for the mass region 1.8–2.0 GeV *and* for $|\vec{p}_t| > 0.25$ GeV, that the probability (predicted by the binomial distribution) of A being opposite in sign to the observation is about a factor of ten smaller than for other regions. There is no reason to believe that A would deviate from zero in the ordinary elastic process. If its spin J_B is not zero, the object B would be produced polarized along the neutrino beam direction, since the incident neutrino is fully polarized. Hence the variation in A in this particular range of mass and $|\vec{p}_t|$ may signify that the polarization direction of B was rotated out of the plane made by ν and p_{tot} through strong interaction with nuclear constituents while traversing the nucleus. Whether this conjecture is true or not will be determined by the accumulation of more statistics. The point is that we should be careful in including events with $|\vec{p}_t|$ greater than 250 MeV/c in the angular distribution analysis, since their kinematics may be distorted by secondary interaction.

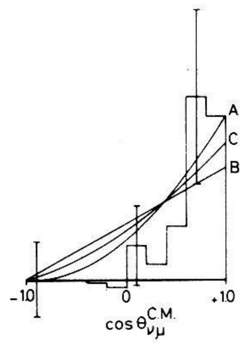

Figure 8
Angular distribution of muons measured from the neutrino direction in *CM* system. Theoretical curves are (A) $(1 + \cos\theta)^2$, (B) $(1 + \cos\theta)$ and (C) the *deceptive* calculation.

In the present data, however, this precaution is hardly necessary because of the very poor statistics. The angular distortions caused by the above effect, which is small anyway, do not reflect upon the angular distribution with any statistical significance. Therefore we present here the angular distribution with full statistics.

Out of 55 events in the 1.8–2.0 GeV mass region, we have subtracted the 33 background events expected. The angular distribution of these subtracted events was determined from the results of the Monte Carlo calculation (Section 3). Figure 8 shows the resultant distribution of $\cos\theta$, where θ is the angle between the incident neutrino direction and the muon direction in the centre of mass.

The observed asymmetry excludes the possibility $J_B = 0$. The value of $\langle\cos\theta\rangle$, the average value of $\cos\theta$, is found to be $0.6 \pm^{0.8}_{0.2}$ (68% confidence level). The value of $\langle\cos\theta\rangle$ is related to the spin of B by an inequality [24, 25],

$$|\langle\cos\theta\rangle| \leqslant \frac{1}{J_B + 1}. \tag{7.1}$$

Thus the rather large value of $\langle\cos\theta\rangle$ suggests $J_B = 1$. In the following we will assume $J_B = 1$.

The highest possible order in $\cos\theta$ in an angular distribution of decay products from a system of spin J is $2J$ when J is integer [26]. For $J = 1$, the angular distribution therefore has the form

$$d\sigma \sim (1 + a\cos\theta + b\cos^2\theta)\, d\Omega. \tag{7.2}$$

The highest asymmetry (ratio of the intensity into the forward hemisphere to that into the backward) corresponds to $a = 2\sqrt{3}$ and $b = 3$ in (7.2). The ratio is then $\sim$14:1. However, this corresponds to a mixture of $J = 1$ and $J = 0$. For pure $J = 1$, the highest asymmetry is obtained when $a = 2$ and $b = 1$, giving a $(1 + \cos\theta)^2$ distribution. In this case, only the $M^{J_B} = -1$ state is populated (i.e. B is fully polarized upstream with respect to the neutrino beam) and the helicity of the final state equals 1. However, if the $M^{J_B} = -1$ and 0 states are equally populated, the distribution is given by $a = 1$ and $b = 0$, or $(1 + \cos\theta)$. On the other hand the calculation of Ref. [8] gives a value of $a = 1.34$ and $b = 0.39$.

These three distributions, $(1 + \cos\theta)^2$, $(1 + \cos\theta)$ and $(1 + 1.34 \cos\theta + 0.39 \cos^2\theta)$ were fitted to the observed distribution with the method of least squares. The results, giving equal statistical weight to each bin, are shown in Figure 8. With proper weights, χ^2, for 9 degrees of freedom, is 5.4 for $(1 + \cos\theta)$, the worst of the three fits. Hence we conclude that there are no fundamental contradictions in our angular distribution with the theoretical predictions.

8. Other Processes

The possible three-body decay modes of a neutral B are $B \to p + \mu^- + \pi^0$ and $B \to n + \mu^- + \pi^+$. However, the presence of a generally undetected π^0 or neutron makes an exact evaluation of the total mass of the three particles difficult because the neutron target is in motion. In mass distributions calculated assuming that the target is at rest, for both the $p\mu^-$ sample with $|\vec{p}_t| > 300$ MeV/c, $\vec{p}_p + \vec{p}_\mu + \vec{p}_{\pi^0}{}^{(\mathrm{cal.})} > 300$ MeV/c, and

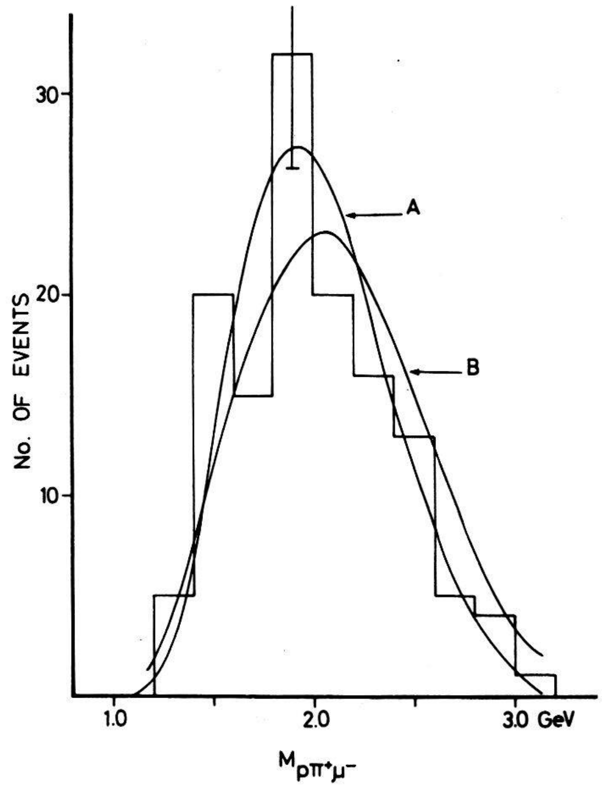

Figure 9
Invariant mass distribution of $p\pi^+\mu^-$ system compared with expected distribution calculated from the cross-section by Veltman and Berman with a double pole form factor [22] and the neutrino spectrum (curve A). Curve B is when the cross-section goes up linearly with the neutrino energy. The samples are chosen from the 1967 $p\pi^+\mu^-$ events with $\sum p_x > 0.3$ GeV/c.

the $\mu^-\pi^+$ sample with the π^+ identified and $\vec{p}_p + \vec{p}_\mu + \vec{p}_n{}^{(\mathrm{cal.})} > 300$ MeV/c, one observes no significant enhancement in the mass region 1.8 to 2.0 GeV.

If B is charged, the decay mode $B^+ \to p + \mu^- + \pi^+$ can exist. The mass distribution of $p\mu\pi^+$ events with $\sum p_x > 0.3$ GeV/c observed in the propane run exhibits a peak at 1.8–2.0 GeV (Fig. 9). However, it can be explained completely within statistics by calculations for N^* production by a number of authors [22].

No statistically significant indication of associated production of B with pions, such as $\nu + p \to B + \pi^+$, $\nu + n \to B + \pi^0$ (using $\mu^- p$ and $\mu^- C$ events failing the tests) or $\nu + n \to B^- + \pi^+$ $(B^- \to n + \mu^-)$, has been observed with our neutrino beam. Recently Campbell et al [29] at ANL have studied $\nu + p \to p + \mu^- + \pi^+$ channel using a hydrogen target. Their neutrino flux is below the 1967 CERN neutrino beam by a factor of five at 1.5 GeV. They concluded that the effect is not seen in this channel. No remark, however, was made on the five events observed in the 1.80–1.84 GeV/c^2 bin, where slightly less than one event is expected (Fig. 2b of Ref. [29]). The probability of finding more than four events in this bin is of the order of 10^{-3} and the centre of the bin, 1.82 GeV/c^2, is less than two standard deviations away from our average mass (0.4 standard deviation away from freon result). It is worth pointing this out although the significance is not established within the Campbell experiment.

Hence the decay modes to these channels, if they exist, are still the subject of further studies. Furthermore an overwhelming dominance of N^* production in these processes is to be noted.

9. Remarks

We ask ourselves how this effect should be interpreted. It may of course be a statistical effect (three standard deviations). It is unlikely to be an instrumental effect because, since the beginning of this experiment (1963), numerous changes have been made in the experimental conditions.

For example, the proton energy, the target, the focusing system, the layout of the shield, the bubble chamber, the liquid in the chamber, the measurement equipment, and the geometrical reconstruction and kinematical fitting programs have all been changed and the net result is an average of these changes.

It is difficult to attribute the effect to any anomaly in the neutrino spectra or to any nuclear effects. It is interesting therefore to consider the possibility that this may be a new type of resonance B between the neutron and the muon–neutrino (Fig. 6) which decays into proton and muon. Let us assume only two decay channels, $n\nu$ and $p\mu$, and that the coupling constants g and g' are the same. Neglecting the spin of the boson and equating the partial widths then gives the following relation at the resonance.

$$\sigma_{\mathrm{res}}^{p\mu} = \frac{\pi \lambdabar^2}{2} = \frac{g^2}{2m\Gamma}, \tag{9.1}$$

where $\sigma_{\mathrm{res}}^{p\mu}$ is the resonance cross-section to the $p\mu$ channel and Γ the total width of the resonance. The observed rate R is related to the observed cross-section σ_{obs}, the observed width Γ_{obs}, and to (9.1) by

$$R = \sigma_{\mathrm{obs}} \Gamma_{\mathrm{obs}} = \sigma_{\mathrm{res}}^{p\mu} \Gamma. \tag{9.2}$$

Since $\Gamma_{\mathrm{obs}} \sim 100$ MeV, $\sigma_{\mathrm{obs}} \sim 10^{-38}$ cm^2 from the elastic background and the gross order of magnitude of $\sigma_{\mathrm{res}}^{p\mu}$ is $\sim 10^{-27}$ cm^2, Γ is of the order of 10^{-3} eV or 10^{-12} sec in life-time.

This is long enough for B to escape the nucleus and decay freely outside of it. The coupling constant, g, is then given by

$$g^2/4\pi \sim 10^{-12}. \tag{9.3}$$

However, this is 10^{-7} times smaller than required for an intermediate scalar boson of this mass mediating the ordinary weak interaction [7].

Consequently, Itami et al. [8], while keeping the relation $gg'/(4\pi m_B^2) = G/\sqrt{2}\pi$, proposed that the ratio of the squares of the coupling constants, g^2/g'^2, could be as small as 10^{-6}, to bring down the resonance cross-section. In this case, $g'^2/4\pi \sim 10^{-3}$ and is as strong as the electromagnetic interaction, but the prediction still exceeds our observation by a factor of 1000. Furthermore, De Rujula and Zia [27] have estimated the upper limit of $g'^2/4\pi$ imposed by the muon $(g-2)$ experiment [28] to be not more than 10^{-4}. Similarly, for the other extreme, $g^2/g'^2 \sim 10^6$, as many as 10^9 neutrons would have been produced even only in our chamber during the whole run. With the neutrons emitted from shield, magnet etc. in addition, our pictures would have certainly been flooded with recoil protons and neutral stars. This was not the case. Thus the assumption $g \cong g'$ is a more likely and natural choice.[4])

In the argument so far we have always used the *total* neutrino flux. The estimation of the cross-section of the resonance, or the magnitude of g and Γ, is entirely based on the assumption that the effect is caused by the full flux of the neutrino beam. One might consider the possibility that the B is coupled only to the neutrinos from kaon decay or to the antineutrino in the background. In the energy region 1–2 GeV, both fluxes are only of the order of 0.1%of the dominant neutrino flux from pion decay and the above numbers would change by a corresponding factor. However, if the B were coupled only to the antineutrino background it would have been extremely prominent in the 1965 antineutrino run. This possibility can therefore be excluded.

Acknowledgments

The author is greatly indebted to Prof. J. S. Bell, Prof. D. H. Perkins and Dr. W. A. Venus. He has gained very much from them through discussions, comments and criticism in the whole course of the present analysis. He is very thankful for their carefully reading the manuscript, making many corrections and pointing out a number of problems. Thanks are due to Drs. A. De Rujula and R. Zia who calculated the effect on the $(g-2)$. The author is thankful to his colleagues of the Heavy Liquid Bubble Chamber Group and for the kind hospitality extended to him by Profs. V. F. Weisskopf and B. P. Gregory, the directors of CERN, and by Dr. C. A. Ramm, the leader of the neutrino experiment.

REFERENCES

Only surnames are listed when the number of authors exceeds five per article.

[1] A. SALAM, Nuovo Cimento *5*, 299 (1957); L. D. LANDAU, Nucl. Phys. *3*, 127 (1957); T. D. LEE and C. N. YANG, Phys. Rev. *105*, 1671 (1957).

[2] E. C. G. SUDARSHAN and R. E. MARSHAK, Phys. Rev. *109*, 1860 (1958); R. P. FEYNMAN and M. GELL-MANN, Phys. Rev. *109*, 193 (1958); J. J. SAKURAI, Nuovo Cimento *7*, 649 (1958).

[3] H. YUKAWA, Proc. Phys. Math. Soc. Japan *17*, 48 (1935); T. D. LEE and C. N. YANG, Phys. Rev. *108*, 1611 (1957).

[4]) *If* we stick to the position of 'deceptive' scheme [8] in the framework of the weak interaction, one of many possibilities is that our observation might be indicating the presence of $V + A$ by a tiny amount in the weak currents. This is suggested by a Fierz transformation on currents such as $\bar{\mu}\gamma_\mu(1+\gamma_5)p^c\,\bar{n}^c\gamma_\mu(1+\gamma_5)\nu$.

[4] Block, Burmeister, Cundy, Eiben, Franzinetti, Keren, Møllerud, Myatt, Nikolic, Lecourtois, Paty, Perkins, Ramm, Schultze, Sletten, Soop, Stump, Venus and Yoshiki, Phys. Letters *12*, 281 (1964).
[5] Burns, Danby, Hyman, Lederman, Lee, Rettberg and Sunderland, Phys. Rev. Letters *15*, 830 (1965); Bernardini, Bienlein, Böhm, von Dardel, Faissner, Ferrero, Gaillard, Gerber, Hahn, Holder, Kaftanov, Krienen, Manfredotti, Reinharz, Salmeron, Staude, Steiner, Bartley, Block, Burmeister, Cundy, Eiben, Franzinetti, Keren, Møllerud, Myatt, Nikolic, Lecourtois, Paty, Perkins, Ramm, Schultze, Sletten, Soop, Stump, Venus, and Yoshiki, Nuovo Cimento *38*, 608 (1965); A new limit, 5.5 GeV, is claimed by a cosmic ray analysis: R. Cowsik and Y. Pal, Int. Conf. on Cosmic Rays, Budapest (1969). The recent NAL experiment suggests this limit as high as 20 G eV (1973).
[6] B. L. Ioffe and E. P. Shabalin, Yadern. Fiz. *6*, 828 (1967), Eng. trans. Soviet Jour. Nucl. Phys. *6*, 603 (1968); S. L. Glashow, H. J. Schwitzer and S. Weinberg, Phys. Rev. Letters *19*, 205 (1967); R. N. Mohapatra, J. S. Rao and R. E. Marshak, Phys. Rev. Letters *20*, 108 (1968); M. Gell-Mann, M. Goldberger, L. Kroll and F. Low, Phys. Rev. *179*, 1518 (1969).
[7] Y. Tanikawa and S. Watanabe, Phys. Rev. *113*, 1344 (1959); T. Kinoshita, Phys. Rev. Letters *4*, 378 (1960); Y. Tanikawa and S. Nakamura, Suppl. Prog. Theor. Phys. *37* and *38*, 306 (1966).
[8] K. Itami, S. Nakamura, N. Mugibayashi and T. Tankiawa, Prog. Theor. Phys. *32*, 301 (1964).
[9] Non-existence of this kind of boson up to 1.5 GeV for electron–proton system was also verified; Allaby, Gittelman, Prepost, Ritson, Coward and Richter, Phys. Rev. *133*, B1514 (1964).
[10] Budagov, Cundy, Franzinetti, Fretter, Hopkins, Manfredotti, Myatt, Nezrick, Nikolic, Novey, Palmer, Pattison, Perkins, Ramm, Roe, Stump, Venus, Wachsmuth and Yoshiki, Let. Nuovo Cimento *2*, 689 (1969).
[11] Budagov, Cundy, Franzinetti, Fretter, Hopkins, Manfredotti, Myatt, Nezrick, Nikolic, Novey, Palmer, Pattison, Perkins, Ramm, Roe, Stump, Venus, Wachsmuth and Yoshiki, Phys. Letters *29B*, 524 (1969)
[12] A. Lecourtois and C. A. Piketty, Nuovo Cimento *50A*, 927 (1967).
[13] Y. Yamaguchi, Prog. Theor. Phys. *23*, 1117 (1960); T. D. Lee and C. N. Yang, Phys. Rev. Letters *4*, 307 (1960); N. Cabibbo and R. Gatto, Nuovo Cimento *15*, 304 (1960).
[14] Allaby, Binon, Diddens, Duteil, Klovning, Meunier, Peigneux, Sacharidis, Schlupmann, Spighel, Stroot, Thorndike and Wetherall (to be published).
[15] S. van der Meer, CERN 61-7 (1961); A. Ašner and Ch. Iselin, CERN 66-24 (1966).
[16] H. Wachsmuth, CERN NPA/Int. 68-20 (1968); Bloes, Pattison, Plass, Rusch, Venus and Wachsmuth, Proc. of CERN Neutrino Meeting 1969 (to be published).
[17] (a) G. Myatt, CERN/NPA/Int. 64-35 (1964); (b) C. Franzinetti and C. Manfredotti, CERN/NPA/Int. 67-30 (1967); (c) C. Manfredotti, CERN/NPA/Int. 68-8 (1968); (d) J. Løvseth, CERN/TH/861 (1967).
[18] Yu. M. Kazarinov, 'The Nucleon–Nucleon and –Nucleon Interaction below 1 GeV', 12th Int. Conf. on High Energy Phys. Dubna (1964); R. Wilson, *The Nucleon–Nucleon Interaction* (Interscience Pub. 1963); D. Cheng, Rev. Mod. Phys. *39*, 526 (1967); E. Lomon and H. Feshbach, Rev. Mod. Phys. *39*, 611 (1967).
[19] G. F. Chew and J. Steinberger, Phys. Rev. *78*, 497 (1950).
[20] V. M. Sidorov, JETP *28*, 727 (1955).
[21] M. Block, S. Passman and W. Havens, Phys. Rev. *88*, 1239 (1952); S. Passman, M. Block and W. Havens, Phys. Rev. *88*, 1247 (1952).
[22] S. Berman and M. Veltman, Nuovo Cimento *38*, 993 (1965); C. H. Albright and L. S. Liu, Phys. Rev. *140B*, 1611 (1965); Ph. Salin, Nuovo Cimento *48*, 506 (1967); S. L. Adler, Ann. Phys. *50*, 189 (1968).
[23] (a)H. Yoshiki, CERN/NPA/Int. 63-30 (1963); (b) H. Yoshiki, CERN/NPA/Int. 64-40 (1964); (c) C. Franzinetti, CERN 66-13, p. 13; (d) D. H. Perkins, CERN 69-7 (1969), p. 9.
[24] T. D. Lee and C. N. Yang, Phys. Rev. *109*, 1755 (1958).
[25] M. Jacob, Nuovo Cimento *9*, 826 (1958).
[26] C. N. Yang, Phys. Rev. *74*, 764 (1948).
[27] A. de Rujula and R. Zia, Nuclear Physics *19B*, 224 (1970).
[28] Bailey, Bartl, Von Bochmann, Brown, Farley, Jöstlein, Picasso and Williams, Phys. Letters *28B*, 287 (1968).
[29] Campbell, Charlton, Cho, Derrick, Engelmann, Fetkovich, Hyman, Jaeger, Jankowski, Mann, Mehtani, Musgrave, Schreiner, Wangler, Whitmore and Yuta, Phys. Rev. Letters *30*, 335 (1972).